

On effect of wave breaking on short wind waves

Vladimir Kudryavtsev^{1,2} and Johnny Johannessen^{3,4}

Received 27 May 2004; accepted 20 September 2004; published 26 October 2004.

[1] The paper presents an attempt to estimate short wave generation by wave breaking. A breaking wave crest disturbs the surface and generates sub-surface turbulence. The locally disturbed area further disperses and feeds short wave energy to the surroundings. The total short wave energy results from summing up the effect of wave breaking events randomly distributed over the sea surface. The rate of short wave generation is determined by the frequency of wavebreaking events per unit area. The source of short wave energy is isotropic, thus it generates waves at cross and opposite wind directions. The model qualitatively reproduces observed directional property of short wind wave spectra and mean square slope. **INDEX TERMS:** 4504 Oceanography: Physical: Air/sea interactions (0312); 0669 Electromagnetics: Scattering and diffraction; 4506 Oceanography: Physical: Capillary waves; 4560 Oceanography: Physical: Surface waves and tides (1255). **Citation:** Kudryavtsev, V., and J. Johannessen (2004), On effect of wave breaking on short wind waves, *Geophys. Res. Lett.*, 31, L20310, doi:10.1029/2004GL020619.

1. Introduction

[2] The sea surface provides radiowave backscattering at any radar look directions in respect to the wind direction. At VV-polarization and moderate incidence angles radar scattering is proportional to wavenumber spectrum of short wind waves (SW) at Bragg wavenumber. Observations show that backscatter is neither vanished nor negligible at cross-wind directions [e.g., Donelan and Pierson, 1987; Carswell *et al.*, 1999]. It presumes that SW travelling cross and opposite wind possess sufficient portion of energy. Moreover, Carswell *et al.* [1999] found that up-wind/cross-wind backscatter ratio rapidly increases at low (<5 m/s) winds, i.e., anisotropy of SW is strongly wind dependent. Banner *et al.* [1989] revealed that in real conditions wavenumber spectra in the wavelength range from 0.2 m to 1.6 m is almost isotropic.

[3] Wind input is the governing source of SW energy. For the SW, the wind growth rate $\beta(\mathbf{k})$ is [e.g., Meirink *et al.*, 2003]

$$\beta(\mathbf{k}) = C_{\beta} \left(u_* / c \right)^2 \cos \varphi |\cos \varphi| \quad (1)$$

where φ is the angle between wind and wave, u_* is air friction velocity, C_{β} is a “constant”, and c is the phase

speed. Thus SW aligned with the wind grow, while they attenuate in the opposite case. The question is what explains the origin of SW travelling opposite to the wind. Three plausible mechanisms may be identified. The first one is random fluctuations in the wind direction (most significant at low winds [e.g., Carswell *et al.*, 1999]) which can generate SW at directions not aligned to the mean flow. The second mechanism is the resonant wave-wave interactions which may redistribute the energy in wavenumber space. Calculations published in literature are always focused on the vicinity of the spectral peak, thus magnitudes of the non-linear energy transfer in the range of SW are not available. We leave this problem out of the scope of the present study. Here we examine the third mechanism, - generation of SW by breaking waves of a larger scale. Such a nonlinear mechanism was considered by Lyzenga [1996]. Using results of laboratory experiment by Walker *et al.* [1996], he proposed an expression for the SW spectrum generated by a stationary breaker. The remaining question is thus how this result can be applied to real breaking waves which are essentially non-stationary and are rare on the sea surface. Recently A. Rozenberg and M. Ritter (Laboratory study of fine structure of the short surface waves due to breaking: Two-directional wave propagation, submitted to *Journal of Geophysical Research*, 2004, hereinafter referred to as Rozenberg and Ritter, submitted manuscript, 2004) found that a non-stationary breaking generates both bound and free gravity-capillary waves. Free waves were found to co- and counter-propagate relative the breaking wave with comparable amplitudes. Their study provides a ground to assume that in real conditions breaking splashes may be treated as the source of SW generation. The goal of the present study is to estimate the rate of SW generation by breaking waves, and to demonstrate the significance of this mechanism.

2. A Simplified Approach

[4] In real condition life span of breakers is much smaller than an interval between successive breaking events at given point. We skip the details of breaking wave evolution (including effect of strong orbital velocity on SW), and consider only its final stage. We assume that generation of SW by breaking waves can be treated within the frame of the classical problem of wave generation by an initial surface perturbation [e.g., Whitham, 1974]. As the initial perturbation we consider a disturbed surface confined within the surface area (with scale l) turned over by a breaking crest. We analyze wave field in the “far zone”, i.e., at a distance significantly exceeding scale l . Due to dissipative processes, the life span of the shortest waves may not be sufficient to reach the far zone. However, in this section we ignore this fact, and consider the energy balance in section 4.

¹Marine Hydrophysical Institute, Sebastopol, Ukraine.

²Also at Nansen Environmental and Remote Sensing Center, Bergen, Norway.

³Nansen Environmental and Remote Sensing Center, Bergen, Norway.

⁴Also at Geophysical Institute, University of Bergen, Norway.

[5] In the far zone wave field possesses the radial symmetry. Solution of this problem at $r \gg l$ reads [e.g., *Whitham*, 1974]:

$$\eta(r, t) = \frac{1}{\sqrt{r}} \frac{\hat{\eta}_0(k_0) \sqrt{k_0}}{\sqrt{t|\omega''(k_0)|}} \cos(k_0 r - \omega t) \quad (2)$$

where r is distance from the initial perturbation (localized at $r = 0$), $\hat{\eta}_0(k)$ is Hankel transform of initial perturbation $\eta_0(r)$, ω is dispersion relation, k_0 is wavenumber satisfying the condition of stationary phase: $\omega'(k_0) = r/t$.

[6] Let us assume that the water surface is disturbed by a large number of initial perturbations randomly distributed over a large area with a surface density n_A . Then $dN = n_A \cdot 2\pi r dr$ is a total number of perturbations confined in the ring of width $dr \ll r$. Each perturbation generates a wave field (2), and the wave energy in the middle of the ring is

$$de = \sum_1^{dN} \overline{\eta_i^2} = \pi n_A |\hat{\eta}_0|^2 k_0 / (t|\omega''|) dr \quad (3)$$

The total wave energy can then be found by integration of (3) over all r . The element dr is related to the wavenumber interval dk of waves passing the given point as: $dr/dk = \omega'' t$. Then, changing the integration variable in (3), we obtain

$$e = \pi n_A \int |\hat{\eta}_0|^2 k dk \quad (4)$$

This equation shows that the total energy is constant in time (waves are free, i.e., there is no energy dissipation yet). If we define wave spectral density $F(k, \varphi)$ as

$$e = \iint F(k, \varphi) k dk d\varphi,$$

then equation (4) shows that

$$F(k) = n_A l^2 F_0(k) \quad (5)$$

where $F_0 = (1/2)l^{-2}|\hat{\eta}_0|^2$ is the spectral density of the initial perturbation per unit surface. Thus, the spectrum of SW corresponds to the spectrum of an initial individual perturbation, and its level is proportional to the number of wavebreaking events per unit surface.

3. Estimate of Rate of SW Energy Generation

[7] Let us assume that at some stage the surface will again be disturbed by the same set of perturbations. Then the total wave energy will be doubled. If this process keeps repeating, the SW energy should experience step-like growth. A random process can be characterized by frequency of perturbations per unit surface n_{AT} . Then one may anticipate that the mean growth rate of wave energy is

$$\partial F / \partial t \equiv S_{wb} = n_{AT} l^2 F_0(k). \quad (6)$$

To define $F_0(k)$, we note that Fourier transform of a steep wave before breaking cannot serve as the spectrum of initial perturbation. Instability of the sea surface develops very fast, and the process of wave crest disruption is accompanied by generation of subsurface turbulence and chaotic enhanced

surface roughness. We may assume that this roughness is isotropic and its spectrum corresponds to the saturated spectrum $F_0 \propto k^{-4}$. *Walker et al.* [1998] measured the spectrum of surface roughness at steady breaking in lab conditions. They found that the spectrum is isotropic, and for large k becomes saturated at $ak^{-3.5}$ with $a = 3 \cdot 10^{-3} m^{1/2}$. From dimensional arguments, the spectrum $F_0 \propto k^{-4}$ is more attractive, and we fitted this spectrum to the experimental data:

$$F_0(k, \varphi) = a / (2\pi) h(k - k_L) k^{-4} \quad (7)$$

where $a = 3 \cdot 10^{-1}$, $h(x)$ is Heaviside step function, which truncates spectrum at wavenumber k_L related to wavenumber of the breaking wave K as: $k_L = a_L K$. According to *Walker et al.* [1996], constant a_L should be of order 10 [see *Walker et al.*, 1996, Figure 7b].

[8] To estimate n_A and n_{AT} , we use wave breaking statistics introduced by *Phillips* [1985]: $\Lambda(\mathbf{K}) d\mathbf{K}$ - total length per unit area of breaking fronts of waves with wavenumbers from \mathbf{K} to $\mathbf{K} + d\mathbf{K}$. Assume that the scale of breaking zone is $l \propto K^{-1}$, the number of breaking zones per unit surface is $n_A \propto K \Lambda(\mathbf{K}) d\mathbf{K}$, and the frequency of wave breaking events per unit area, correspondingly, is $n_{AT} \propto K \Omega \Lambda(\mathbf{K}) d\mathbf{K}$, where Ω is the frequency of breaking wave. Then the energy source (6) becomes

$$dS_{wb}(k, K) \propto a / (2\pi) k^{-4} h(k - k_L) C \Lambda(\mathbf{K}) d\mathbf{K} \quad (8)$$

$C = \Omega / K$ is the phase speed. Integrating (8) over \mathbf{K} , we define the rate of SW generation by all breaking waves:

$$S_{wb}(k) = \int dS_{wb} \propto a / (2\pi) k^{-4} \int_0^{K_m} C \Lambda(\mathbf{K}) d\mathbf{K} \quad (9)$$

where the upper limit of integration K_m is: $K_m = \min(k/a_L, k_{wb})$, k_{wb} is the wave number of the shortest gravity waves which can be disrupted at wave breaking process. Shorter breaking waves with $K > k_{wb}$, due to the effect of surface tension, are not disrupted, but produce "regular" trains of parasitic capillaries (bound waves). An estimate of k_{wb} is: $k_{wb} \approx 2\pi/0.3$ rad/m. A spectral model of generation of the parasitic capillaries as well as references to previous studies are given by *Kudryavtsev et al.* [2003].

[9] One of the advantages of the wave breaking statistics in terms of Λ is that it is related to the energy dissipation $D = b g^{-1} C^5 \Lambda(\mathbf{K})$, where b is a constant of order 0.01 [*Phillips*, 1985]. To define D we have to adopt an assumption on the energy balance. As shown below, the main contribution to S_{wb} results from breaking waves, which belong to the equilibrium range. There are two opposite approaches to the problem of energy balance in this range. The first approach presumes that breaking waves balance the non-linear energy flux (the Kolmogorov type cascade) from the range of energy containing waves. The second approach presumes that dissipation due to breaking is proportional to the energy input from wind $g\beta\Omega K^{-4} B(\mathbf{K})$, where B is the saturation spectrum [*Phillips*, 1985]. For the present estimates we follow the second approach. Then

$$\Lambda(\mathbf{K}) \propto b^{-1} K^{-1} \beta B(\mathbf{K}) \quad (10)$$

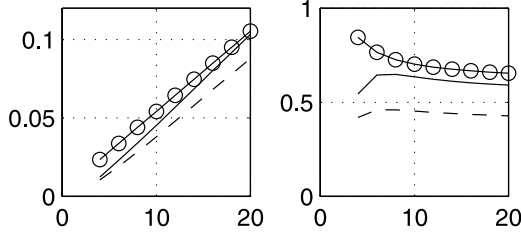


Figure 1. Total mean square slope $s_{up}^2 + s_{cr}^2$ (left plot) and ratio s_{cr}^2/s_{up}^2 (right plot) of cross- and up-wind components versus wind speed. Open circles are empirical relations by *Cox and Munk* [1954]; dashed line calculations are based on the reference spectrum (term I_{wb} in (13) is omitted); solid lines show calculations based on the full spectrum.

and the source term (9) becomes

$$S_{wb}(k) \propto a/(2\pi b)k^{-4} \iint_{K < K_m} \Omega \beta B(\mathbf{K}) d \ln K d\varphi \quad (11)$$

This equation relates the SW energy source to the wind energy input to longer waves. It does not depend on φ and predicts SW generation at cross and opposite wind directions. Notice, that integral in (11) converges very fast at the upper limit. It means that the main contribution to S_{wb} comes from the shortest breaking waves, while the role of dominant waves breaking is weak.

4. Short Wave Energy Balance

[10] At uniform conditions, the sources and sinks of energy in the equilibrium range are balanced so that

$$\beta_\nu E - D - S_N + (\omega^2/k)(S_{wb} + S_{pc}) = 0 \quad (12)$$

where $\beta_\nu = \beta(\mathbf{k}) - 4\nu k^2/\omega$ is the effective growth rate; ν is the molecular viscosity coefficient; $E = \omega^2 k^{-5} B$ is the spectral energy density; $D = b g^{-1} C^5 \Lambda$ is the energy losses due to wave breaking; S_N is the resonant wave-wave interactions; S_{pc} is the rate of generation of parasitic capillaries, and S_{wb} is defined by (11). Solution of this equation (with parameterized Λ and S_N) gives a shape of the wave spectrum. To emphasize the role of S_{wb} we adopt the same parameterization of Λ and S_N as by *Kudryavtsev et al.* [2003]. In this case, the energy balance (12) reads

$$\beta_\nu(\mathbf{k})B(\mathbf{k}) - B(\mathbf{k})[B(\mathbf{k})/\alpha]^n + I_{pc}(\mathbf{k}) + I_{wb}(k) = 0 \quad (13)$$

where I_{wb} is the dimensionless wave breaking source (11)

$$I_{wb}(k) = c_b/(2\pi\omega) \iint_{K < K_m} \Omega \beta B(\mathbf{K}) d \ln K d\varphi, \quad (14)$$

c_b is a new constant adopting a and b in (11); I_{pc} is the rate of generation of parasitic capillaries (bound waves) by small-scale wave breaking written in the form proposed by *Kudryavtsev et al.* [2003]:

$$I_{pc}(\mathbf{k}) = \beta(\mathbf{k}_g)B(\mathbf{k}_g)\phi(k/k_\gamma), \quad (15)$$

$k_g = k_\gamma^2/k$ is the wave number of the gravity wave which generates the parasitic capillary wave at wavenumber k ; k_γ is the wave number of the minimum phase velocity ($k_\gamma \approx 370$ rad/m), ϕ is a filter function which is close to 1 at $2 < k/k_\gamma < k_\gamma/k_{wb}$ and vanishes outside. The second term in (13) describes the non-linear energy losses which are caused by wavebreaking (at $k/k_\gamma \ll 1$), generation of parasitic capillaries (at $k_{wb} < k < 1/2k_\gamma$), and three-wave interactions (at $k/k_\gamma \propto 1$). Parameters α and n in (13) are functions of k/k_γ (see *Kudryavtsev et al.* [2003] for more details). Equation (13) can be solved numerically with respect to $B(\mathbf{k})$.

[11] First, we consider approximate solutions of (13) at $k/k_\gamma < 1$ (where $I_{pc} = 0$). In the wind direction, I_{wb} should be small in comparison with the wind input, thus

$$B(\mathbf{k}) \approx \alpha[\beta_\nu(\mathbf{k})]^{1/n}. \quad (16)$$

This spectrum model was proposed earlier by *Donelan and Pierson* [1987]. At cross wind directions (or at φ where $\beta_\nu(\mathbf{k}) \approx 0$), the SW spectrum is

$$B(\mathbf{k}) \approx \alpha[I_{wb}(k)/\alpha]^{1/(n+1)}. \quad (17)$$

At opposite wind directions (where $\beta_\nu(\mathbf{k}) < 0$), the non-linear dissipation in (13) can be ignored (since B is small), and the SW spectrum is:

$$B(\mathbf{k}) \approx -I_{wb}(k)/\beta_\nu(\mathbf{k}) \quad (18)$$

This spectrum results from the balance of the wave breaking source and the energy losses due to viscosity and SW interaction with opposing wind.

5. Some Model Estimates and Comparison With Data

[12] The wave breaking source (14) is defined with accuracy of the constant c_b . We estimate c_b through comparison of the model ratio of cross-wind (s_{cr}^2) and up-wind (s_{up}^2) mean square slopes of the sea surface with *Cox and Munk* [1954] observations. Dashed lines in Figure 1 show the mean square slope $s_{cr}^2 + s_{up}^2$ and the ratio s_{cr}^2/s_{up}^2 as a function of wind speed calculated for the wave spectrum without accounting for I_{wb} in (13) (hereinafter, reference spectrum). Open circles correspond to the empirical relation by *Cox and Munk* [1954]. Reference calculations slightly underestimate $s_{cr}^2 + s_{up}^2$ and significantly underestimate s_{cr}^2/s_{up}^2 . Solid lines indicate the model calculations based on the full spectrum. In these calculations, the proportionality constant in (14) is $c_b = 0.75$. Accounting for I_{wb} results in an increase of anisotropy of mean square slope components. This value of c_b gives also a reasonable agreement of the model with radar observation (see Figure 4 below), and is thus adopted in further calculations.

[13] The directional distributions of $B(\mathbf{k})$ for k 's related to radar wavenumbers of P-, L-, C-, and Ku-bands (wavelengths 70, 23, 5.3, and 2 cm respectively) at wind speed of 10 m/s are shown in Figure 2. The reference spectra (Figure 2a) are vanished at cross and opposite wind directions. The wave breaking energy source, however, pumps the energy into all directions. In the wind direction, this impact is negligible (compare Figure 2a and Figure 2b). At cross and

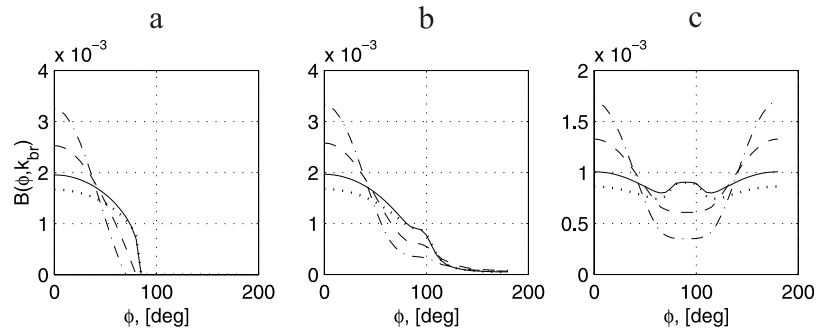


Figure 2. Directional distributions of wave spectra for a wind speed of 10 m/s at wave numbers corresponding to P-band (dotted lines), L-band (solid lines), C-band (dashed lines), and Ku-band (dashed-dotted lines). a)- directional reference spectra; b)- directional full spectra; c)- folded spectra corresponding to directional spectra in plot b).

opposite wind directions, however, generation of SW by breaking waves plays a crucial role. Folded wavenumber spectra related to the directional wavenumber spectra as $1/2(B(\mathbf{k}) + B(-\mathbf{k}))$ are shown in Figure 2c. For the shortest waves, the folded spectra keep up a well-pronounced directionality, while for gravity waves with the wavelengths of 23 and 70 cm they are almost isotropic. This qualitatively corresponds to experimental findings of *Banner et al.* [1989].

[14] Omni-directional saturation spectra for wind speeds 5, 10 and 20 m/s are shown in Figure 3. Comparing with the reference spectra, we conclude that contribution of the wave breaking is noticeable. The wave spectra at $k > 2k_\gamma \approx 740$ rad/m are mainly defined by the mechanism of generation of parasitic capillaries (term I_{pc} in (13)). Generation of this type of short bound waves by breaking surface was observed e.g., by Rozenberg and Ritter (submitted manuscript, 2004). Generation of “free” capillary wave by large scale breaking waves (described by I_{wb} in (13)) is weak.

[15] Field observations of up-wind to cross-wind ratio of the normalized radar cross section (NRCS) at VV polarization for different radar frequencies and wind speeds from 8 to 12 m/s are shown in Figure 4. At moderate incidence angles, the NRCS is proportional to the SW folded spectrum at Bragg wavenumber. Radar data demonstrate an existence of wave energy at cross-wind directions.

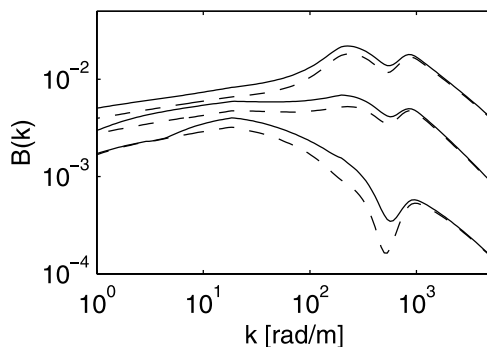


Figure 3. Omni-directional saturation spectra at 5, 10, and 20 m/s wind speeds (curves of the same style from the bottom to the top). Dashed lines are the reference spectra, solid lines are the full spectra.

The directional spreading narrows as the radar wave number increases. The model calculations correctly reproduce the measurements. Some underestimate (on 1dB) at lowest radar frequencies and overestimate at Ku-band is, however, apparent. As it was discussed by *Kudryavtsev et al.* [2003], the latter may be attributed to the influence of a non-Bragg scattering mechanism.

6. Conclusion

[16] A breaking wind wave generates both subsurface water turbulence and enhanced surface roughness. Subsequently, the localized induced roughness disperses and feeds short wave energy to the surroundings. The rate of short wave generation is then determined by the frequency of occurrence of wavebreaking events per unit area, and depends on the spectral density of induced roughness inside the breaking zone. The source of short wave energy due to the breaking waves is isotropic. Thus, this mechanism (in contrast to the wind generation) generates waves at cross- and opposite-to-the-wind directions. This effect may thus explain the radar observations showing presence of the short wave energy at cross-wind directions.

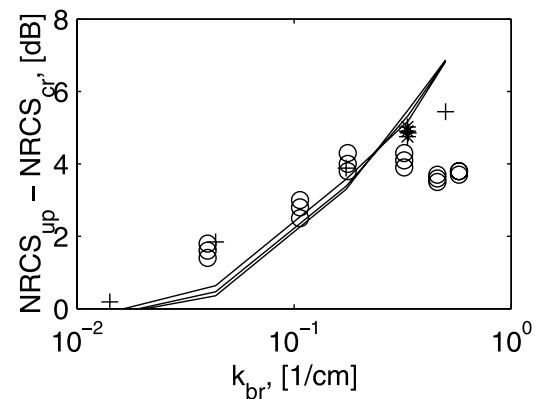


Figure 4. Upwind-to-crosswind ratio as a function of inverse radar wavelength, for VV polarization, at incidence angle of 30° and wind speeds of 8, 10 and 12 m/s. Solid lines are model calculations. Symbols are radar observations (for notation, see *Kudryavtsev et al.* [2003, Figure 9]).

[17] **Acknowledgments.** We acknowledge the support by the Norwegian Space Center (under the contract JOP.8.3.3.10.02.2) and by the EU INTAS under projects INTAS –01-234. V. K. acknowledges the support by the Office of Naval Research under grant N00014-03-1-0619 (PR NO.: 03PR09880-00).

References

- Banner, M. L., I. S. F. Jones, and J. C. Trinder (1989), Wavenumber spectra of short gravity waves, *J. Fluid. Mech.*, 65, 647–656.
- Carswell, J. R., W. D. Donnelly, and R. E. McIntosh (1999), Analysis of C and Ku band backscatter measurements under low-wind conditions, *J. Geophys. Res.*, 104, 20,687–20,701.
- Cox, C., and W. Munk (1954), Measurements of the roughness of the sea surface from photograms of the Sun's glitter, *J. Opt. Soc. Am.*, 44, 838–850.
- Donelan, M. A., and W. J. Pierson (1987), Radar scattering and equilibrium ranges in wind-generated waves with application to scatterometry, *J. Geophys. Res.*, 92, 4971–5029.
- Kudryavtsev, V., D. Hauser, G. Caudal, and B. Chapron (2003), A semiempirical model of the normalized radar cross-section of the sea surface, I. Background model, *J. Geophys. Res.*, 108(C3), 8054, doi:10.1029/2001JC001003.
- Lyzenga, D. R. (1996), Effects of wave breaking on SAR signatures observed near the edge of the Gulf Stream, in *IGARSS '96: 1996 International Geoscience and Remote Sensing Symposium: Remote Sensing for a Sustainable Future*, vol. II, pp. 908–910, IEEE Press, Piscataway, N. J.
- Meirink, J.-F., V. Makin, and V. Kudryavtsev (2003), Note on the growth rate of water waves propagating at an arbitrary angle to the wind, *Boundary Layer Meteorol.*, 106, 171–183.
- Phillips, O. M. (1985), Spectral and statistical properties of the equilibrium range in the wind-generated gravity waves, *J. Fluid Mech.*, 156, 505–531.
- Walker, D. T., D. R. Lyzenga, E. A. Ericson, and D. E. Lung (1996), Radar backscatter and surface roughness measurements from stationary breaking waves, *Proc. R. Soc. London, Ser. A*, 452, 1953–1984.
- Whitham, G. B. (1974), *Linear and Nonlinear Waves*, 622 pp., Wiley-Interscience, Hoboken, N. Y.

J. Johannessen, Nansen Environmental and Remote Sensing Center, Edvard Griegsvei 3a, N-5059 Bergen, Norway.

V. Kudryavtsev, Marine Hydrophysical Institute, Ukrainian Academy of Sciences, 2 Kapitanskaya St., Sevastapol 335000, Ukraine.